



*Dedicated to Professor Cristian Silvestru  
on the occasion of his 65th anniversary*

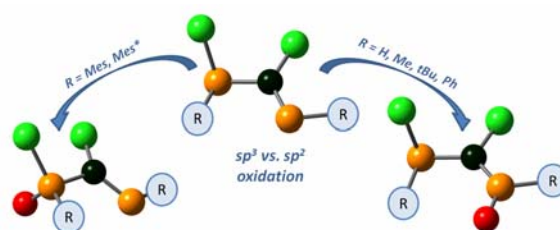
## OXIDATION OF $sp^2$ VERSUS $sp^3$ PHOSPHORUS ATOM IN 1,3-DIPHOSPHAPROPENES. A DFT STUDY

Ionut-Tudor MORARU, Raluca SEPTLEAN and Gabriela NEMES\*

Faculty of Chemistry and Chemical Engineering, Department of Chemistry, METALOMICA Research Centre, Babeş-Bolyai University, 11 Arany Janos, 400028 Cluj-Napoca, ROUMANIA

Received October 31, 2019

DFT calculations are performed on the diphosphapropene model  $RP=C(Cl)-P(Cl)R$  ( $R = H, Me, Ph, tBu, Mes, Mes^*$ ) in order to understand the selectivity of the  $sp^2$  versus  $sp^3$  phosphorus atoms towards oxidation. The two reaction mechanisms investigated in this respect aim at evaluating the roles played by the bulkiness of the R group on the computed kinetic and thermodynamic parameters. In addition, NBO techniques are employed in order to compute charges and bond orders for the investigated species.



### INTRODUCTION

The chemistry of the diphosphaalkene derivatives has undergone a continuous development and maintains its interest, not only from the point of view of the fundamental knowledge but also due to the applications of these compounds, especially in obtaining coordinative species with applications in catalysis. In this respect 1,3-diphosphapropene  $Mes^*P=C(Cl)-PRR'$  or 3-thio-1,3-diphosphapropene  $Mes^*P=C(Cl)-P(=S)R$  ( $Mes^* = 2,4,6$ -triterbutylphenyl) were prepared and used as monodentate or chelating ligands.<sup>1</sup> In some cases the obtained coordinative compounds containing palladium or platinum atom display catalytic activities for the Sonogashira and Suzuki cross-coupling reactions.<sup>2</sup>

Closer to our research interest are the studies regarding the use of diphosphapropene derivatives

containing the  $P=C-P$  or  $P=C-P=E$  moieties ( $E = S$  or  $O$ ) as precursors for the synthesis of some heterocumulenes of  $P=C=P$  or  $P=C=P=E$  types. If in the case of symmetric carbodiphosphirane  $R_3P=C=PR_3$  a large number of compounds have been described in the literature,<sup>3</sup> the chemistry of unsymmetrical diphosphaallenes containing a bicoordinated trivalent and a tricoordinated pentavalent phosphorus atom (namely the  $P=C=P(=E)$  backbone when  $E$  is a group 16 element) is still mostly unknown.<sup>4</sup> These unsaturated phosphorus compounds are interesting mainly from the fundamental point of view, many questions such as the determination of the geometry, the charges, the electronic configuration, the types of substituents (electron releasing or withdrawing) able to stabilize the double bonds need an answer. Regarding the stabilization of the  $P=C$  unsaturated bond in diphosphapropenes or

\* Corresponding authors: [gabriela.nemes@ubbcluj.ro](mailto:gabriela.nemes@ubbcluj.ro)

diphosphaallenes, it is known that the use of bulky organic groups on the phosphorus atoms induce adequate kinetic effects to afford stable species.<sup>4,5</sup> An additional stabilization can be induced by the oxidation of the phosphorus atoms from P(III) to P(V). In most of the cases reported so far, and even in great excess of the oxidized agent (DMSO or sulfur), reactions occur preferentially at the  $sp^3$  phosphorus atom.<sup>1,2,5</sup>

Furthermore, a series of theoretical studies were performed in order to explain the nature of the chemical bonds, and the effects of the substituents on the stabilization of the low coordinated phosphalkenyl derivatives. For instance, *ab initio* calculations have been reported for the  $XP=C=PX$  ( $X = H, F, Cl$ ) symmetric systems<sup>6</sup> or for unsymmetrical ones such as  $HP=C=NH$  or  $HP=C=O$ <sup>7</sup> in order to explain the effect of the substituents on the stability of this type of derivatives, the conformational stability or electronic structures. Some theoretical study were performed on the  $H_2CP_2O$  systems in order to determine the possible isomers including the 1,3-diphosphaallene model  $HP=C=P(=O)H$ .<sup>8</sup> This study revealed that even though the isomers containing the  $P=C=P=O$  skeleton do not have the lowest relative energy their stabilization can be achieved by including the adequate steric hindrance on the phosphorus atoms. An additional study shows that the electronic effect is also important in the stabilization of such compounds.<sup>9</sup> For example the silyl group linked on the P(V) atom increase the stability of derivatives  $RP=C=P(=O)R$ , while the presence of electron-withdrawing groups destabilizes the diphosphaallenic systems.

Considering all the above mentioned aspects, we herein present a DFT study aiming to understand the selectivity of the  $sp^2$  versus  $sp^3$  phosphorus atoms towards oxidation with dimethylsulfoxide (DMSO). For this purpose, we assessed the oxidation mechanisms of several  $RP=C(Cl)-P(Cl)R$  models ( $R = H, Me, Ph, tBu, Mes, Mes^*$ ), in order to understand how the bulkiness of the R substituents impacts the reactivity of these species.

## RESULTS AND DISCUSSION

For carrying out the DFT study on the oxidation reactions of diphosphapropenes models  $RP=C(Cl)-P(Cl)R$  ( $R = H, Me, Ph, tBu, Mes, Mes^*$ ) we consider only species with the same R group on both sides of the  $P=C-P$  unit. A schematic representation of the possible oxidation routes of the model diphosphapropenes discussed herein is

illustrated in Figure 1, the two possibilities involving either the oxidation of the  $sp^3$  P atom, or the oxidation of the  $sp^2$  P atom of the  $C=P$  double bond.

Selected geometrical features obtained from the DFT calculations performed on the model  $RP=C(Cl)-P(Cl)R$  species are presented in Table 1. The computed values of the P-C-P angles and of the P=C and C-P bonds display similar values among the series considered throughout this text and additionally they are in line with previously published data on similar systems.<sup>10</sup> For instance, experimental determined structure of  $Mes^*P=C(Cl)-PPh_2$  reveals P-C-P angles of  $104^\circ$  and P=C and C-P distances of 1.67 Å and 1.78 Å respectively, highlighting thus a good correlation between theory and crystallographic data (Table 1). The bond orders for the P=C and C-P bonds were computed using the Natural Resonance Theory (NRT) within the framework of the Natural Bond Orbital (NBO) analysis. The values displayed in Table 1 indicate that the bond orders of the P=C bonds among the investigated series range in-between 1.67-1.83, being slightly lower than the expected value of 2, while for the C-P bonds, the calculated NRT bond orders reveal values that are slightly higher than 1 in all cases (1.06-1.13). Concerning the computed charges (NPA charges were considered throughout this text) for the atoms of the  $P=C-P$  unit, values indicate an increased electrophilic behavior for the two P atoms, and a highly negative value on the C atom.

The DFT structures of the oxidized diphosphapropenes  $RP=C(Cl)-P(=O)(Cl)R$  (product **a**,  $P=C-P=O$ ) and  $RP(=O)=C(Cl)-P(Cl)R$  (product **b**,  $O=P=C-P$ ) are also discussed herein. Some key structural features are displayed in Table 2. Computed values of the P-C-P bonding angles and of the P=C and C-P distances for the oxidized products **a** and **b** are resembling to a great extent the values calculated for the corresponding diphosphapropene reactants (see Tables 1 and 2 for comparisons). Nonetheless, in the case of products **b**, calculated P-C-P angles are wider than those of their model reactant counterparts with about  $5-12^\circ$ , featuring an increasing tendency towards widening of the P=C-P angle upon oxidation at the  $sp^2$  P atom. Calculated P=O distances are also displayed, the computed lengths being found to be the same within  $1/100$  Å among the investigated series, while NRT bond orders reveal a multiple bond character in all of the investigated cases (P=O bond order ranges in-between 1.29 and 1.68).

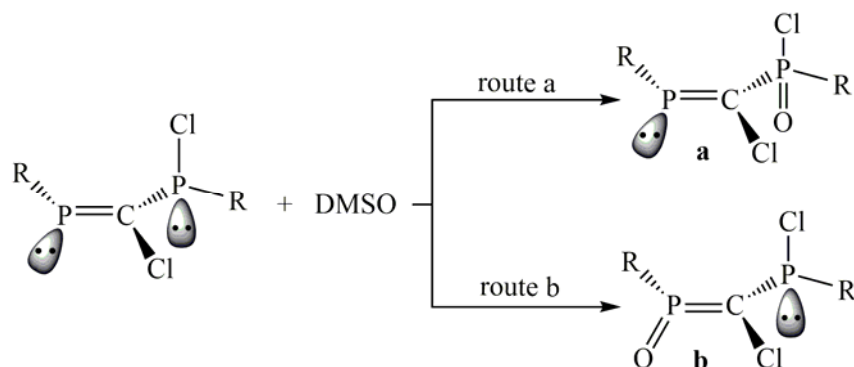


Fig. 1 – Schematic representation of the possible routes for the oxidation reaction of  $RP=C(Cl)-P(Cl)R$  model species ( $R = H, Me, Ph, tBu, Mes, Mes^*$ ). The two possibilities involving the different P atoms of the P=C-P unit are depicted; **route a**: oxidation occurring at the  $sp^3$  P atom, **route b**: oxidation reaction occurring at the  $sp^2$  P atom.

Table 1

Selection of calculated geometrical parameters for  $RP=C(Cl)-P(Cl)R$  species. NPA charges for the C and P atoms of the P=C-P moiety. Computed NRT bond order for the C=P and C-P chemical bonds are additionally displayed

R	P-C-P (°)	C-P (Å)	P=C (Å)	$q_C$	$q_P(sp^3)$	$q_P(sp^2)$	NRT C-P	NRT P=C
H	119.3	1.816	1.677	-0.816	0.613	0.459	1.06	1.83
Me	122.4	1.817	1.677	-0.852	0.858	0.701	1.09	1.74
Ph	120.7	1.823	1.681	-0.851	0.869	0.746	1.04	1.70
tBu	124.5	1.833	1.674	-0.857	0.863	0.711	1.12	1.81
Mes	120.4	1.817	1.683	-0.853	0.865	0.720	1.13	1.67
Mes*	121.4	1.821	1.683	-0.892	0.866	0.748	-	-

Table 2

Selected structural features for system **a** (P=C-P=O) and **b** (O=P-C-P). NRT bond orders are also presented for the C-P, P=C and P=O chemical bonds

R	Product	P-C-P (°)	C-P (Å)	P=C (Å)	P=O	NRT C-P	NRT P=C	NRT P=O
H	a	117.0	1.805	1.674	1.462	0.76	1.84	1.66
	b	123.9	1.799	1.649	1.466	1.08	1.36	1.68
Me	a	120.9	1.809	1.673	1.465	0.77	1.76	1.68
	b	129.5	1.805	1.653	1.470	1.00	1.40	1.66
Ph	a	118.8	1.812	1.678	1.467	0.93	1.95	1.29
	b	124.8	1.809	1.657	1.469	1.01	1.68	1.34
tBu	a	122.2	1.828	1.671	1.469	0.79	1.85	1.64
	b	133.8	1.820	1.658	1.476	1.11	1.39	1.63
Mes	a	119.0	1.814	1.677	1.468	0.93	1.96	1.30
	b	129.6	1.807	1.659	1.471	1.04	1.68	1.32
Mes*	a	118.4	1.822	1.678	1.472	-	-	-
	b	132.9	1.807	1.661	1.472	-	-	-

Concerning the reactivity of the  $RP=C(Cl)-P(Cl)R$  diphosphapropenes towards oxidation with DMSO, mechanistic studies were performed in this respect. The two oxidation mechanisms investigated (routes **a** and **b**) are illustrated in Figure 2 for the particular cases of  $R = Ph$  and  $R =$

$Mes^*$ . Moreover, the calculated reaction enthalpies and activation barriers of the two pathways are displayed in more detail in Table 3, for all of the investigated  $RP=C(Cl)-P(Cl)R$  model species considered herein. According to the computed reaction enthalpies for routes **a** and **b**,  $\Delta H(\mathbf{a})$  and

$\Delta H(\mathbf{b})$ , the oxidation reactions are highly exothermic in both cases, the formation of oxidized products **a** and **b** being thus expected, in line with our previous experimental findings<sup>1f</sup>. However, the calculated energy differences between  $\Delta H(\mathbf{a})$  and  $\Delta H(\mathbf{b})$  are significantly high in all cases, the oxidation of the  $sp^3$  P atom being thermodynamically favored in all cases with calculated gaps of 9.5-16.5 kcal mol<sup>-1</sup> (Table 3). Regarding the activation energies ( $E_a$ ) computed for the two oxidation schemes **a** and **b**, DFT calculations reveal a common trend for both pathways: activation barriers increase with the increasing bulkiness of the R substituent (Table 3). On the other hand, calculations highlight that for  $RP=C(Cl)-P(Cl)R$  species containing small R groups (H, Me, Ph, *t*Bu) the oxidation route **b** is kinetically favored (activation barriers are with 8.7-11.6 kcal mol<sup>-1</sup> lower than those computed for route **a**), whereas increasing the bulkiness of the R substituents (Mes, Mes\*) changes the kinetic control towards route **a** (Table 3). The general outcome of this mechanistic study stresses the effect played by the R group of  $RP=C(Cl)-P(Cl)R$  diphosphapropenes on their reactivity towards oxidation. Thus, in the case of small substituents (R = H, Me, Ph, *t*Bu) the kinetic product  $RP(=O)=C(Cl)-P(Cl)R$  (route **b**) is favored, while for bulkier groups (R = Mes, Mes\*) formation of the  $RP=C(Cl)-P(=O)(Cl)R$  species (route **a**) is preferred from both kinetic and thermodynamic viewpoints. These results are better summarized in Figure 2, which illustrates the different reactivity trends for the particular cases of  $PhP=C(Cl)-P(Cl)Ph$  (small substituent) and  $Mes^*P=C(Cl)-P(Cl)Mes^*$  (bulky protecting group) models.

Finally, we assess the structural features of the optimized transition state (TS) species. The calculated TS structures for pathways **a** (**TS\_a**) and **b** (**TS\_b**) are illustrated in Figure 3 as a particular case for the oxidation reaction of the  $MeP=C(Cl)-P(Cl)Me$  derivative. Within **TS\_a**, the oxygen atom of DMSO coordinates to the  $sp^3$  phosphorus atom from opposite direction with respect to the P-Cl bond. In the particular case of R = Me (Figure 3a), the calculated O-P-Cl angle is of 163.7°, while the P-O distance is of 1.736 Å and a computed NRT bond order of 0.79. DFT calculations also suggest a slight elongation of the P-Cl bond upon oxidation, the bond distance stretching with about 0.183 Å with respect to the equilibrium geometry. Concerning the S-O chemical bond (of DMSO), calculations indicate a significant elongation upon coordination to the P atoms, from 1.481 Å (NRT bond order = 1.27) in DMSO to 1.816 Å (NRT bond order = 0.53) in the TS structure. Furthermore, NBO analyses reveal that the lone pair electrons (LP) on the P atom lies in the same plane with the  $C(Cl)=PR$  moiety and the methyl group (Figure 3). As a general remark, the **TS\_a** structures optimized for the other models considered throughout this text display similar features. For example, calculated O-P-Cl angles and P-O bond lengths among the investigated series range in-between 159.5-166.3°, and 1.704-1.760 Å respectively. For the **TS\_b** optimized geometries, DFT calculations reveal a trigonal pyramidal geometry around the phosphorus atom in all cases, with the coordination of the oxygen atom to the  $sp^2$  phosphorus one, distorting the initial planar arrangement.

Table 3

Calculated enthalpies of reaction ( $\Delta H$ ) and activation enthalpies ( $E_a$ ) for the oxidation reaction pathways depicted in Figure 2 for model diphosphapropenes  $RP=C(Cl)-P(Cl)R$ . Calculated energy gaps between the reaction enthalpies of the two routes ( $\Delta_b H - \Delta_a H$ ), and between the activation barriers of route **a** and **b** ( $E_a(\mathbf{b}) - E_a(\mathbf{a})$ ) are displayed

R	H	Me	Ph	<i>t</i> Bu	Mes	Mes*
$\Delta_a H$ (kcal mol <sup>-1</sup> )	-36.5	-42.0	-41.6	-43.0	-39.5	-35.2
$E_a$ (route <b>a</b> ) (kcal mol <sup>-1</sup> )	23.7	25.6	25.5	28.4	28.1	36.9
$\Delta_b H$ (kcal mol <sup>-1</sup> )	-21.9	-26.8	-25.2	-27.8	-25.1	-25.7
$E_a$ (route <b>b</b> ) (kcal mol <sup>-1</sup> )	14.6	15.2	13.9	19.7	30.9	40.3
$\Delta_b H - \Delta_a H$ (kcal mol <sup>-1</sup> )	<b>14.6</b>	<b>15.2</b>	<b>16.4</b>	<b>15.3</b>	<b>14.4</b>	<b>9.5</b>
$E_a(\mathbf{b}) - E_a(\mathbf{a})$ (kcal mol <sup>-1</sup> )	<b>-9.1</b>	<b>-10.4</b>	<b>-11.6</b>	<b>-8.7</b>	<b>2.8</b>	<b>3.8</b>

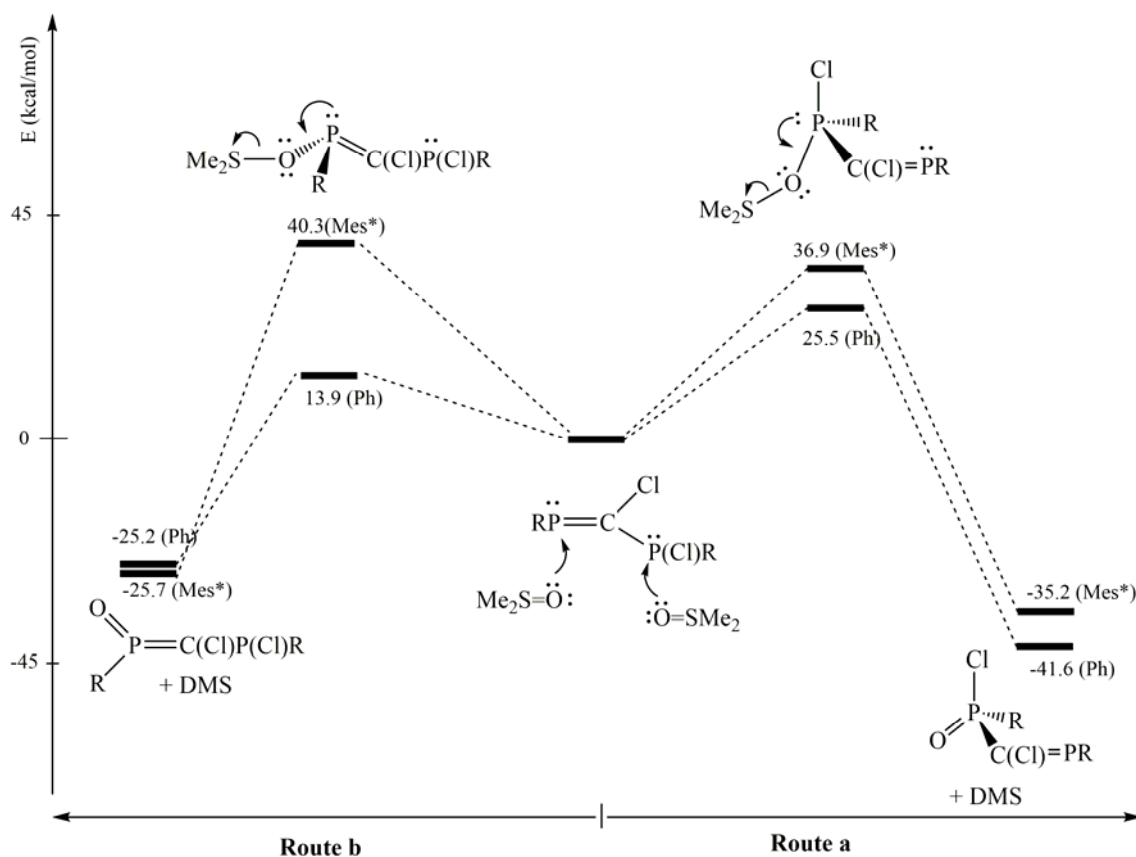


Fig. 2 – Oxidation mechanisms for derivatives  $\text{PhP}=\text{C}(\text{Cl})\text{-P}(\text{Cl})\text{Ph}$  and  $\text{Mes}^*\text{P}=\text{C}(\text{Cl})\text{-P}(\text{Cl})\text{Mes}^*$ . Route **a**: oxidation of the  $sp^3$  P atom. Route **b**: oxidation of the  $sp^2$  P atom. Computed reaction enthalpies and activation barriers are illustrated. A schematic representation of the investigated geometries (reactants, products, transition states) is also suggested.

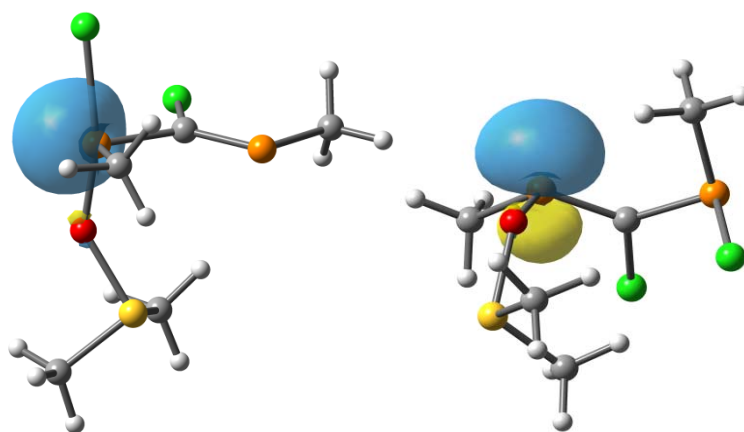


Fig. 3 – Transition state structures optimized for the oxidation reaction of model  $\text{MeP}=\text{C}(\text{Cl})\text{-P}(\text{Cl})\text{Me}$  species. **a**. TS geometry for oxidation reaction occurring at the  $sp^3$  P atom; **b**. TS structure corresponding to the oxidation of the  $sp^2$  P atom. The lone pair electrons on the  $sp^3$  and  $sp^2$  phosphorus atoms are also displayed. Atomic color legend: H – white; C – grey; O – red; P – orange; S – yellow; Cl – green.

For the particular case of  $\text{R} = \text{Me}$  (Figure 3b), the calculated P-O bond distance is of 1.629 Å and a corresponding NRT bond order of 1.11, while for the S-O bond (from the coordinated DMSO) the computed length is of 1.906 Å and the NRT bond order is of 0.58. Moreover, NBO techniques reveal a mainly  $p$  lone pair (90%  $p$ , 10%  $s$ ) for the P

atom. Similar values are also obtained for the other **TS\_b** model species considered herein.

### Computational details

All calculations were performed within the framework of the Density Functional Theory

(DFT), using the *Gaussian 09* package.<sup>11</sup> The molecular geometries were fully optimized in the gas phase without any symmetry constraints, and employed the PBE0<sup>12</sup> hybrid functional, and the valence triple-zeta Def2-TZVP<sup>13</sup> basis set. The optimization criteria were set to tight in all cases. Vibrational analyses were performed in order to characterize the nature of the stationary points. Additionally, frequency calculations were used to compute reaction and activation enthalpies. The integration grid used was of 99 radial shells and 950 angular points for each shell (99,950), more precisely the “ultrafine” grid within *Gaussian 09*. Natural Bond Orbital (NBO)<sup>14</sup> analyses were carried out on the optimized structures of the investigated species. Charges were computed within the framework of the Natural Population Analysis (NPA) of the NBO theory. Bond orders were obtained from Natural Resonance Theory (NRT) analyses available in NBO calculations. For all NBO analyses performed herein, the *NBO 7.0 Program*<sup>15</sup> was employed.

## CONCLUSIONS

DFT calculations were carried out on model RP=C(Cl)-P(Cl)R diphosphapropenes (R = H, Me, Ph, *t*Bu, Mes, Mes\*) in order to understand their reactivity towards oxidation with DMSO. Two mechanisms are investigated in this respect, evaluating the oxidation selectivity between the  $sp^3$  P atom (route **a**, formation of RP=C(Cl)-P(=O)(Cl)R species), and the  $sp^2$  one (route **b**, formation of RP(=O)=C(Cl)-P(Cl)R products). In all calculated cases, formation of the RP=C(Cl)-P(=O)(Cl)R product (route **a**) is thermodynamically favored with 9.5 to 16.5 kcal mol<sup>-1</sup>. However, in the case of small R substituents (H, Me, Ph, *t*Bu), formation of the RP(=O)=C(Cl)-P(Cl)R kinetic product (route **b**) is expected, as computed activation energies for route **b** are significantly lower than those corresponding to route **a** (calculated gaps of -8.7 to -11.6 kcal mol<sup>-1</sup>). In the case of sterically hindered RP=C(Cl)-P(Cl)R models (R = Mes, Mes\*), route **a** (oxidation occurring at the  $sp^3$  P atom) is favored from both kinetic and thermodynamic viewpoints. Finally, another trend emerges from DFT calculation: oxidation barriers increase with the increasing bulkiness of the R group, for both  $sp^3$  and  $sp^2$  phosphorus atoms.

*Acknowledgements.* This work was supported by a grant of Ministry of Research and Innovation, CNCS – UEFISCDI, project number PN-III-P4-ID-PCE-2016- 0351, within PNCDI

III, Roumania. We are also grateful for computational resources which were provided by the high-performance computational facility of the Babes-Bolyai University (MADECEP, POSCCE, COD SMIS 48801/1862) co-financed by the European Regional Development Fund of the European Union.

## REFERENCES

- (a) M. Yoshifuji, K. Toyota and N. Inamoto, *J. Chem. Soc., Chem. Commun.*, **1984**, 689–690; (b) R. Appel, P. Fölling, B. Josten, M. Siray, V. Winkhaus and F. Knoch, *Angew. Chem. Int. Ed. Engl.*, **1984**, *23*, 618–619; (c) M. Gouygou, M. Koenig, J. Escudié and C. Coureat, *Heteroat. Chem.*, **1991**, *2*, 221–227; (d) M. Yoshifuji, S. Sasaki and N. Inamoto, *J. Chem. Soc., Chem. Commun.*, **1989**, 1732–1733; (e) S. Ito, K. Nishide and M. Yoshifuji, *Organometallics*, **2006**, *25*, 1424–1430; (f) R. Septelean, G. Nemes, J. Escudie, I. Silaghi-Dumitrescu, H. Ranaivonjatovo, P. Petrar, H. Gornitzka, L. Silaghi-Dumitrescu and N. Saffon, *Eur. J. Inorg. Chem.*, **2009**, *5*, 628–654.
- (a) H. Liang, S. Ito and M. Yoshifuji, *Org. Lett.*, **2004**, *6*, 452–427; (b) S. Ito, H. Liang and M. Yoshifuji, *J. Organomet. Chem.*, **2005**, *690*, 2531–2535.
- (a) F. Ramires, N. B. Desai, B. Hansen and N. McKelvie, *J. Am. Chem. Soc.*, **1961**, *83*, 3539–3540; (b) J. S. Driscoll, D. W. Grisley Jr., J. V. Pustinger, J. E. Harris and C. N. Matthews, *J. Org. Chem.*, **1964**, *29*, 2427–2431; (c) H. Schmidbaur and A. Schier, *Angew. Chem., Int. Ed.*, **2013**, *52*, 176–186.
- R. Septelean, H. Ranaivonjatovo, G. Nemes, J. Escudie, I. Silaghi-Dumitrescu, H. Gornitzka, L. Silaghi-Dumitrescu and S. Massou, *Eur. J. Inorg. Chem.*, **2006**, 4237–4241.
- (a) S. Ito and M. Yoshifuji, *Chem. Commun.*, **2001**, 1208–1209; (b) H. Liang, K. Nishide, S. Ito and M. Yoshifuji, *Tetrahedron Lett.*, **2003**, *44*, 8297–8300; (c) S. Ito, H. Liang and M. Yoshifuji, *Chem. Commun.*, **2003**, 398–399; (d) K. Nishide, H. Liang, S. Ito and M. Yoshifuji, *J. Organomet. Chem.*, **2005**, *690*, 4809–4815.
- (a) M. T. Nguyen and A. F. Hegarty, *J. Chem. Soc., Perkin Trans. 2*, **1985**, 2005–2012; (b) N. J. Fitzpatrick, D. F. Brougham, P. J. Groarke and M. T. Nguyen, *Chem. Ber.*, **1994**, *127*, 969–978.
- (a) M. Yoshifuji, T. Niitsu, K. Toyota, N. Inamoto, K. Hirotsu, Y. Odagaki, T. Higuchi and S. Nagase, *Polyhedron*, **1988**, *7*, 2213–2216; (b) M. T. Nguyen, A. F. Hegarty, M. A. McGinn and F. J. Ruelle, *Chem. Soc., Perkin Trans. 2*, **1985**, 1991–1997.
- R. Septelean, P.-M. Petrar, G. Nemes, J. Escudie and I. Silaghi-Dumitrescu, *J. Mol. Model.* **2011**, *17*, 1719–1725.
- R. A. Septelean, P. M. Petrar, G. Nemes, J. Escudié and I. Silaghi-Dumitrescu, *Phosphorus Sulfur.*, **2011**, *186*, 2321–2331; (b) R. Septelean, P. M. Petrar and G. Nemes, *Studia UBB Chemia*, **2011**, *54*, 131–141.
- H. Liang, S. Ito and M. Yoshifuji, *Z. Anorg. Allg. Chem.*, **2004**, *630*, 1177–1180.
- M. J. Frisch, G. W. Trucks, H. B. Schlegel, G. E. Scuseria, M. A. Robb, J. R. Cheeseman, G. Scalmani, V. Barone, G. A. Petersson, H. Nakatsuji, X. Li, M. Caricato, A. Marenich, J. Bloino, B. G. Janesko, R. Gomperts, B. Mennucci, H. P. Hratchian, J. V. Ortiz, A. F. Izmaylov, J. L. Sonnenberg, D. Williams-Young, F.

- Ding, F. Lipparini, F. Egidi, J. Goings, B. Peng, A. Petrone, T. Henderson, D. Ranasinghe, V. G. Zakrzewski, J. Gao, N. Rega, G. Zheng, W. Liang, M. Hada, M. Ehara, K. Toyota, R. Fukuda, J. Hasegawa, M. Ishida, T. Nakajima, Y. Honda, O. Kitao, H. Nakai, T. Vreven, K. Throssell, J. A. Montgomery, Jr., J. E. Peralta, F. Ogliaro, M. Bearpark, J. J. Heyd, E. Brothers, K. N. Kudin, V. N. Staroverov, T. Keith, R. Kobayashi, J. Normand, K. Raghavachari, A. Rendell, J. C. Burant, S. S. Iyengar, J. Tomasi, M. Cossi, J. M. Millam, M. Klene, C. Adamo, R. Cammi, J. W. Ochterski, R. L. Martin, K. Morokuma, O. Farkas, J. B. Foresman and D. J. Fox, *Gaussian 09, revision E.01*; Gaussian, Inc.: Wallingford, CT, **2009**.
12. C. Adamo and V. Barone, *J. Chem. Phys.*, **1999**, *110*, 6158-6170.
13. a) A. Schafer, C. Huber and R. Ahlrichs, *J. Chem. Phys.*, **1994**, *100*, 5829; b) D. Rappoport and F. Furche, *J. Chem. Phys.*, **2010**, *133*, 134105.
14. a) F. Weinhold and C. R. Landis, "Valency and Bonding: A Natural Bond Orbital Donor-Acceptor Perspective"; Cambridge Univ. Press: Cambridge, U.K., 2005; b) F. Weinhold and C. R. Landis, "Discovering Chemistry with Natural Bond Orbitals", Wiley-Interscience: Hoboken, NJ., 2012; c) F. Weinhold, C. R. Landis and E. G. Glendening, *Int. Rev. Phys. Chem.*, **2016**, *35*, 399.
15. E. D. Glendening, J. K. Badenhoop, A. E. Reed, J. E. Carpenter, J. A. Bohmann, C. M. Morales, P. Karafiloglou, C. R. Landis and F. Weinhold, *NBO 7.0*, Theoretical Chemistry Institute, University of Wisconsin, Madison, **2018**.

